The effect of stretching thiyl– and ethynyl–Au molecular junctions

2008 J. Phys.: Condens. Matter 20 025207

(http://iopscience.iop.org/0953-8984/20/2/025207)

J. Phys.: Condens. Matter **20** (2008) 025207 (9pp) doi:10.1088/0953-8984/20/02/025207

The effect of stretching thiyl– and ethynyl–Au molecular junctions

R C Hoft[1], M J Ford[1,3], V M García-Suárez[2], C J Lambert[2] and M B Cortie[1]

[1] Institute for Nanoscale Technology, University of Technology Sydney, PO Box 123, Broadway NSW 2007, Australia
[2] Department of Physics, Lancaster University, Lancaster LA1 4YB, UK

E-mail: mike.ford@uts.edu.au

Received 20 August 2007, in final form 1 November 2007
Published 6 December 2007
Online at stacks.iop.org/JPhysCM/20/025207

Abstract
We perform density functional theory (DFT) calculations of the stretching of Au(111)–X–Au(111) molecular junctions where X is either a thiyl or ethynyl biradical. The equilibrium geometries for the radicals adsorbing on the surface are first calculated and the radicals then placed in the junction geometry. The unit cell is stepwise increased in length and the geometry relaxed at each step. When stretching the ethynyl junction, a single gold atom is detached from the rest of the surface and the gold–carbon bond does not break. In contrast, the gold–sulfur bond in the thiyl junction breaks without detaching any gold atoms. This behaviour can be attributed to the enhanced strength of the Au–C interaction over the Au–S interaction. In both junctions the conductance calculated using the non-equilibrium Green's function formalism (NEGF) decreases as the junction is stretched. After breakage of the Au–S bond, the thiyl radical contains an unpaired electron on the sulfur atom and the system is in a spin doublet state. Transmission spectra were calculated for the spin-unpolarized case only; evaluation of the spin-polarized density of states suggests that an enhanced conductance for electrons of one spin type may be observed after the Au–S bond is broken.

1. Introduction

The field of molecular electronics is concerned with ultimately manufacturing usable devices based on molecular circuitry [1]. Elements such as wires and transistors are to be composed of single molecules or a small collection of molecules. While the manufacturing of such devices is still a long-term goal, there are doubts as to their viability, especially due to massive heat dissipation [2].

There have been, however, impressive advances in both experimental characterization of molecular junctions—the fundamental component that needs to be understood in order to build larger systems—and in computational techniques for calculating the transport characteristics of such systems [3].

One prevalent issue regarding the experimental and computational progress has been the apparent mismatch between the absolute values of the current or conductance measured for a particular system. These discrepancies are not confined to comparison between experimental and computational results; indeed, experimental conductance measurements on decanedithiol junctions over the years have yielded results spanning some seven orders of magnitude [4]. It has been clearly established that the system probed cannot be thought of as purely the molecule in question; rather, the conductance properties arise for the system as a whole—the molecule, the leads to which it is attached and the nature of this attachment. Our knowledge of the molecular-level geometry in experiments is uncertain and provides a natural explanation for the range of conductance results observed. In some scanning tunnelling microscopy (STM) experiments there exists a gap between the STM tip and the top of the molecular self-assembled monolayer (SAM). This lack of chemical bonding on one end of the junction will lead to much lower conductance [5]. Even when both ends of the molecule are strongly bound to the respective 'electrodes', the nature of the interface can be quite varied—a typical example is one or more metal adatoms that may protrude from the flat metal surface. Such considerations can alter the measured conductance significantly [6–15].

[3] Author to whom any correspondence should be addressed.

Other issues relating to the overestimation of conductivity by density functional theory (DFT) based calculations have also been investigated; some concern the inadequacy of the static and only approximately correlated nature of the theory to account for transport phenomena properly [16, 17], while others deal with flaws inherent to DFT [18].

Ever-advancing computational and experimental techniques are improving the reproducibility of results [3]. The issue of modelling different junction geometries is however still a topic of considerable interest, not only to reconcile experimental and computational results, but also to obtain an understanding of the mechanics involved in typical experiments and how this may affect results.

The experimental technique which is currently receiving the most attention was pioneered by Tao [19]. It is essentially an STM experiment, with the novel approach that the tip is driven into a substrate in a solution of the molecules under study. The tip is extracted and conductance measurements taken at various intervals. Steps in the conductance trace can be seen, which correspond to conductance values of individual wires. The key idea is that thousands of these measurements lead to construction of conductance histograms with peaks that correspond to statistically significant conductance values. Peaks were identified at integer multiples of a fundamental value, which can be attributed to the conductance of a single gold chain between the substrate and the tip. Similarly, series of lower peak values could be attributed to the conductance of integer multiples of individual molecules. This was the clearest evidence thus far that the conductance of a single small organic molecule could be directly measured.

The nature of the experiment raises interest over the mechanics of stretching and breaking a molecular junction and how the conductance evolves through this process. Early indications were that unexpected behaviour can occur, with Xue and Ratner [15] and Ke *et al* [9] finding an *increase* in conductance as the sulfur–gold distance is stretched beyond the equilibrium value. This was attributed to the relevant molecular energy levels moving closer to alignment with the Fermi level, thereby facilitating resonant tunnelling. Ferry *et al* predicted an increase in conductance when the molecule as a whole is stretched while still attached to both electrodes [13, 14]. This was explained by the delocalization of the molecular orbitals upon stretching, again facilitating the tunnelling process. Romaner *et al* [11] calculated the band structure of a stretched junction, and found that the highest occupied molecular orbital (HOMO) shifts upward into alignment with the metal Fermi level, thus supporting the result of Xue and Ratner. They performed DFT calculations simulating the stretching of a gold–benzenedithiol–gold junction and found that the gold–sulfur bond breaks before detaching a chain of gold atoms from the surface, contrary to the Carr-Parrinello molecular dynamics simulations of Kruger *et al* [20]. However, it was pointed out that the energy difference between the two scenarios is very small and hence the actual stretching behaviour may depend strongly on the initial geometry.

In our previous work [7], we investigated the process of pulling one gold electrode away from the sulfur atom at one end of a thiyl molecular junction. We predicted an increase in conductance upon decoupling of the sulfur with the gold surface, also due to the alignment of the molecular energy levels with the Fermi level. Spin-polarized calculations revealed that the spin doublet state due to the unpaired spin-α electron on the sulfur atom leads to spin splitting of the energy levels. The spin-β levels were then aligned with the Fermi level and the junction in theory acts as a type of spin-filter, with a large transmission coefficient for spin-β electrons, and exponentially decaying coefficient for spin-α electrons.

In the present work, we perform a series of geometry optimizations at intermediate stretching distances of two Au(111)–X–Au(111) junctions, where X is one of benzenedimethanethiol (XYL) or diethynylbenzene (DEB). At selected geometries we calculated the transmission coefficient, to track the evolution of the conductance as the junctions were stretched. Importantly, we have also relaxed the molecular and surface geometry at each step as the two electrodes are pulled apart.

2. Method

2.1. Geometry relaxations

All geometry optimizations in this work were performed with the SIESTA package [21, 22]. This code implements a self-consistent solution to the electronic structure problem using density functional theory within periodic boundary conditions. The valence electrons are described by a linear combination of numerical atom-centred basis sets and the nucleus plus core electrons represented by norm-conserving pseudopotentials, generated according to the scheme of Troullier and Martins [23] in this work, though in principle any norm-conserving pseudopotentials can be used. A key feature of this code is the finite extent of the numerical basis functions in real space. A cut-off distance for all functions is defined by an 'energy shift' parameter, which specifies the increase in energy of the orbital, due to its confinement.

In this work, we use the generalized gradient approximation (GGA) as parametrized by Perdew *et al* [24] for the exchange–correlation functional. The basis functions used vary somewhat, but our general rule is to use double-ζ plus single-polarization functions for each valence orbital and a 5 mRy energy shift parameter. This corresponds to confinement radii of 2.6–3.8 Å for the various orbitals. We will alert the reader when our basis sets deviate from this default setting. The real-space mesh used for the calculation of the charge density and evaluation of real-space integrals is defined by a 'mesh cut-off' parameter, defining the maximum energy of plane waves that can be represented on the mesh without aliasing. This parameter was set to 300 Ry for all calculations.

The optimization of atomic coordinates is achieved through the BGFS algorithm, with the geometry taken as relaxed when the maximum component of the force on any atom does not exceed 0.04 eV Å^{-1}. We use our previous optimizations of the benzenedimethanethiol and ethynylbenzene molecules on the Au(111) surface as starting points. The unit cell in the plane of the surface contains 3×3

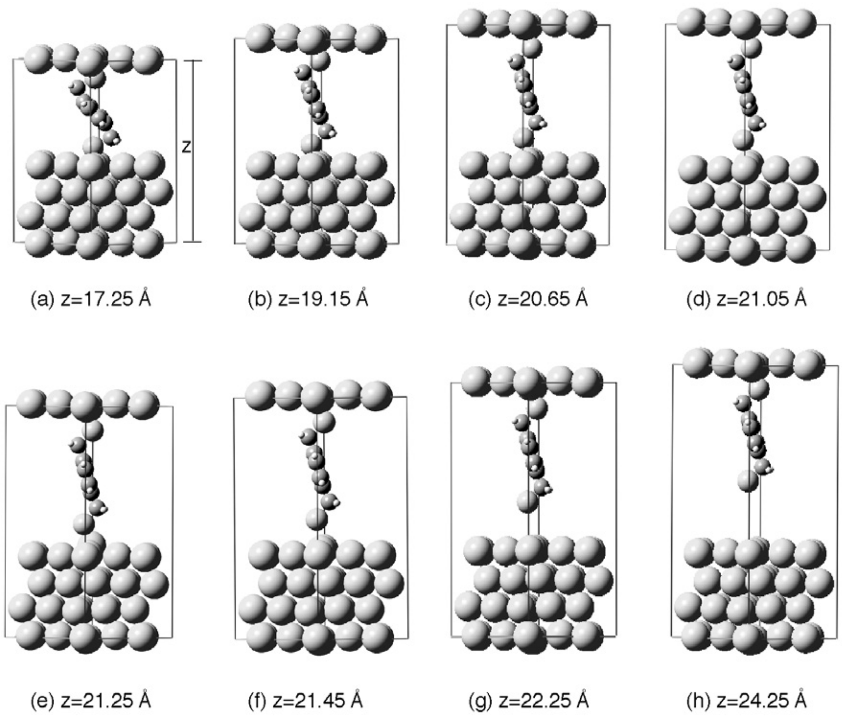

Figure 1. Unit cells of the Au(111)–XYL–Au(111) geometry at selected intervals of stretching. The equilibrium junction geometry is shown in panel (b) with the unit cell length in the direction of transport, $z = 19.15$ Å.

gold atoms, which is enough to prevent the molecules from interacting with their periodic images. The periodicity in this plane is sampled with a Monkhorst–Pack grid [25] of 5×5 k-points in reciprocal space. A four-layer gold slab is used throughout to model the (111) surface. The ability to obtain accurate geometries with the parameters described above has been demonstrated previously [26].

In order to reduce the size of the calculation (in terms of the number of atoms) the unit cell has been set up such that the two electrodes are formed from a single slab. One end of the molecule is adsorbed to the upper side of this slab, while the other end is adsorbed to the under-side of the periodic image of the slab. The equilibrium geometries are given in figures 1(b) and 5(b). The various stages of stretching are achieved by simply increasing the z-length of the unit cell in steps of 0.2–0.5 Å. Optimization is performed, at each step, by allowing the molecule and the top and bottom gold layers (i.e. the gold surface layers) to relax, while keeping the middle two gold layers fixed.

All the SIESTA calculations are spin polarized (spin unrestricted) to take account of the unpaired electron which will remain on the thiol molecule when it's bond with the surface is broken (the terminal hydrogen has been removed from the sulfur headgroup).

2.2. Transport calculations

At selected stages, the transmission function of the junction is calculated with the SMEAGOL package [27, 28]. This is achieved by the non-equilibrium Green's functions (NEGF) technique [29]. Currently, this package is built on the SIESTA code and implements a novel technique for calculating the Green's functions of the metallic leads. The details of this methodology are beyond the scope of the present paper and are described in [27, 28]. Briefly, the retarded self-energies of the two leads are calculated from the *surface* Green's functions of the leads according to equations (7) and (8) of [27].

The self-energies of the leads, Σ_1 and Σ_2, can then be calculated and added to the charge-density dependent device Hamiltonian, $H[\rho]$, to obtain an effective Hamiltonian, H_{eff}. The pertinent quantity for calculating the conductance of the junction is the associated retarded Green's function

$$G^{\mathrm{R}}(E) = \left[\varepsilon^+ S - H - \Sigma_1(E) - \Sigma_2(E)\right]^{-1} \qquad (1)$$

with S the overlap matrix and $\varepsilon^+ = E + \mathrm{i}\delta$. The low-bias conductance for each spin channel ($\sigma = \alpha, \beta$) is calculated as [27]

$$G_\sigma = \frac{e^2}{h}\mathrm{Tr}\left[\Gamma_1 G^{\mathrm{R}+}\Gamma_2 G^{\mathrm{R}}\right]_\sigma (E_F) \qquad (2)$$

with the coupling terms given by

$$\Gamma_{1,2}(E) = \mathrm{i}\left[\Sigma_{1,2}(E) - \Sigma_{1,2}^+(E)\right]. \qquad (3)$$

3. Results and discussion

The optimal geometries for the molecules on the Au(111) surface have been reported previously for benzenedimethanethiol [7] and ethynylbenzene [26]. For completeness we point out that in [7] we used the local density approximation (LDA) for the exchange–correlation potential, whereas in this work

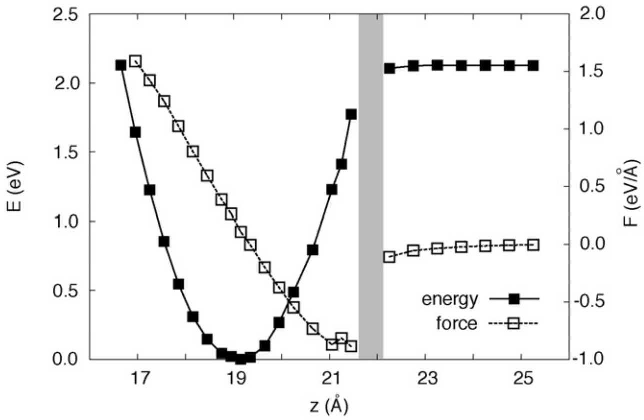

Figure 2. Relative total energy, E, and force, $F = -\mathrm{d}E/\mathrm{d}z$, versus unit cell length z, for the XYL junction. The shaded region indicates the range of z-values where the system is not in a pure spin state.

we use GGA. The binding geometry of benzenedimethanethiol on the Au(111) surface is largely unaffected and attaches with the sulfur atom slightly offset from the bridge towards the fcc site at a height of 2.1 Å above the surface (compared with 2.0 Å in [7]). The terminal carbon atom of ethynylbenzene binds at a height of 1.32 Å above the fcc site. The interaction energies of benzenedimethanethiol and ethynylbenzene with the Au(111) surface are 30 kcal mol^{-1} and 69 kcal mol^{-1} respectively.

3.1. Au(111)–XYL–Au(111) junction

On optimization of the initial junction geometry (figure 1(b)) the XYL molecule stretches slightly. The heights of the sulfur atoms above the respective surfaces are reduced from the single-surface adsorption height to $d_1 = d_2 = 1.9$ Å. Decreasing the length of the unit cell, z, along the transport direction (and hence the interelectrode distance) causes the SCC angles on the methanethiol endgroups to tighten as the sulfur atoms are pushed towards the phenyl ring and the ring becomes more tilted (figure 1(a)).

When the interelectrode distance is increased, the two gold atoms (Au_{1a} and Au_{1b}) bonded to the lower sulfur atom (S_1) are initially pulled out of registry with the rest of the surface. However, the gold–sulfur bond breaks before any gold atoms are detached from the surface. Subsequently, Au_{1a} and Au_{1b} return to registry with the rest of the surface. The system remains in a spin singlet state as the Au–S bond is initially stretched, $z \leqslant 21.45$ Å. Once the bond is broken, the system is in a spin doublet state, $z \geqslant 22.25$ Å, with an unpaired α-spin electron on S_1. For 21.45 Å $< z <$ 22.25 Å, the system is not in a pure spin state and multi-configurational methods are needed for a proper description.

Just prior to breaking of the Au–S bond, the junction is stretched 2.3 Å beyond the equilibrium value. At this point the height of S_1 above Au_{1a} and Au_{1b} is $d_1 = 2.69$ Å, while Au_{1a} and Au_{1b} are out of registry by $\Delta Au_1 = 0.48$ Å. The sulfur (S_2) on the other side of the junction stays attached to the gold surface. Nevertheless, at $z = 21.45$ Å, S_2 has moved to a height of $d_2 = 2.07$ Å above the two gold atoms (Au_{2a} and Au_{2b}) to which it is bonded and Au_{2a} and Au_{2b} have moved out of registry by $\Delta Au_2 = 0.26$ Å.

When the Au–S bond is stretched, the S–C–C angles of the endgroups increase and the phenyl ring tilts towards the surface normal. After the bond is broken, the molecule returns to its equilibrium configuration. The geometric parameters at each stage of the stretching process are summarized in table 1.

Figure 2 shows the total energy, $E(z)$, and the force, $F = -\mathrm{d}E/\mathrm{d}z$, acting on the junction under stress. The force is obtained directly from the SIESTA calculation. Since the z-axis is normal to the base of the unit cell, the force can be calculated as $F = A(\sigma_{zz} - R)$, where A is the xy-area of the unit cell and σ_{zz} is the zz-component of the stress tensor given by SIESTA. R is the residual stress inside the slab as a result of fixing the middle slab layers and is not associated with the junction stretching. R can be found as the limiting value of σ_{zz} once the S–Au bond is broken, $R = \lim_{z\to\infty} \sigma_{zz} = 0.17$ eV Å^{-1}. Because the residual stress is subtracted out, the zero in the force curve does not correspond

Table 1. Geometric parameters for relaxed XYL junctions. d_1 is the height of the sulfur above the two gold atoms to which it is bonded on the lower side of the molecule. ΔAu_1 is the height of these two gold atoms above the rest of the surface. d_2 and ΔAu_2 are similarly defined on the upper end of the molecule. z_{S-S} is the distance between the sulfur atoms on opposite ends of the molecule along the z-axis. θ_{SCC} is the angle made between the sulfur and carbon on the lower methanethiol endgroup and the carbon to which it is bonded on the ring.

z (Å)	d_1 (Å)	ΔAu_1 (Å)	ΔAu_2 (Å)	d_2 (Å)	z_{S-S} (Å)	θ_{SCC} (deg)
16.65	1.75	−0.07	−0.04	1.76	5.97	90.7
16.95	1.77	−0.06	−0.04	1.78	6.22	92.6
17.25	1.79	−0.06	−0.03	1.80	6.47	94.4
17.55	1.79	−0.05	−0.02	1.82	6.73	96.2
17.85	1.81	−0.03	0.00	1.84	6.96	98.6
18.15	1.83	−0.02	0.02	1.87	7.17	100.5
18.45	1.83	−0.01	0.04	1.90	7.40	102.7
18.75	1.85	0.02	0.07	1.93	7.61	105.0
18.95	1.85	0.03	0.08	1.95	7.76	106.8
19.15	1.91	0.08	0.09	1.95	7.84	108.7
19.35	1.93	0.12	0.11	1.97	7.95	109.9
19.65	1.96	0.16	0.15	1.99	8.11	112.0
19.95	2.08	0.22	0.16	1.99	8.22	114.6
20.25	2.13	0.31	0.17	2.01	8.34	116.8
20.65	2.17	0.41	0.24	2.06	8.49	118.3
21.05	2.23	0.50	0.26	2.08	8.62	120.8
21.25	[a]	[a]	0.30	2.12	8.57	119.2
21.45	2.69	0.48	0.26	2.07	8.63	122.0
22.25	4.18	0.14	0.33	1.98	8.22	116.5
22.75	4.75	0.12	0.31	1.98	8.19	116.1
23.25	5.27	0.13	0.31	1.97	8.18	116.0
23.75	5.79	0.12	0.30	1.97	8.16	115.8
24.25	6.30	0.12	0.29	1.97	8.16	115.8
24.75	6.80	0.12	0.29	1.97	8.16	115.8
25.25	7.31	0.12	0.29	1.97	8.15	115.7

[a] In the relaxed geometry for $z = 21.25$ Å, the two gold atoms closest to S_1 move out of registry with each other. One of them is strongly bound to S_1, with distances below S_1 and above the rest of the slab of $d_{11} = 2.0$ Å and $\Delta Au_{11} = 1.0$ Å. The other moves closer to the surface, with $d_{12} = 2.8$ Å and $\Delta Au_{12} = 0.2$ Å.

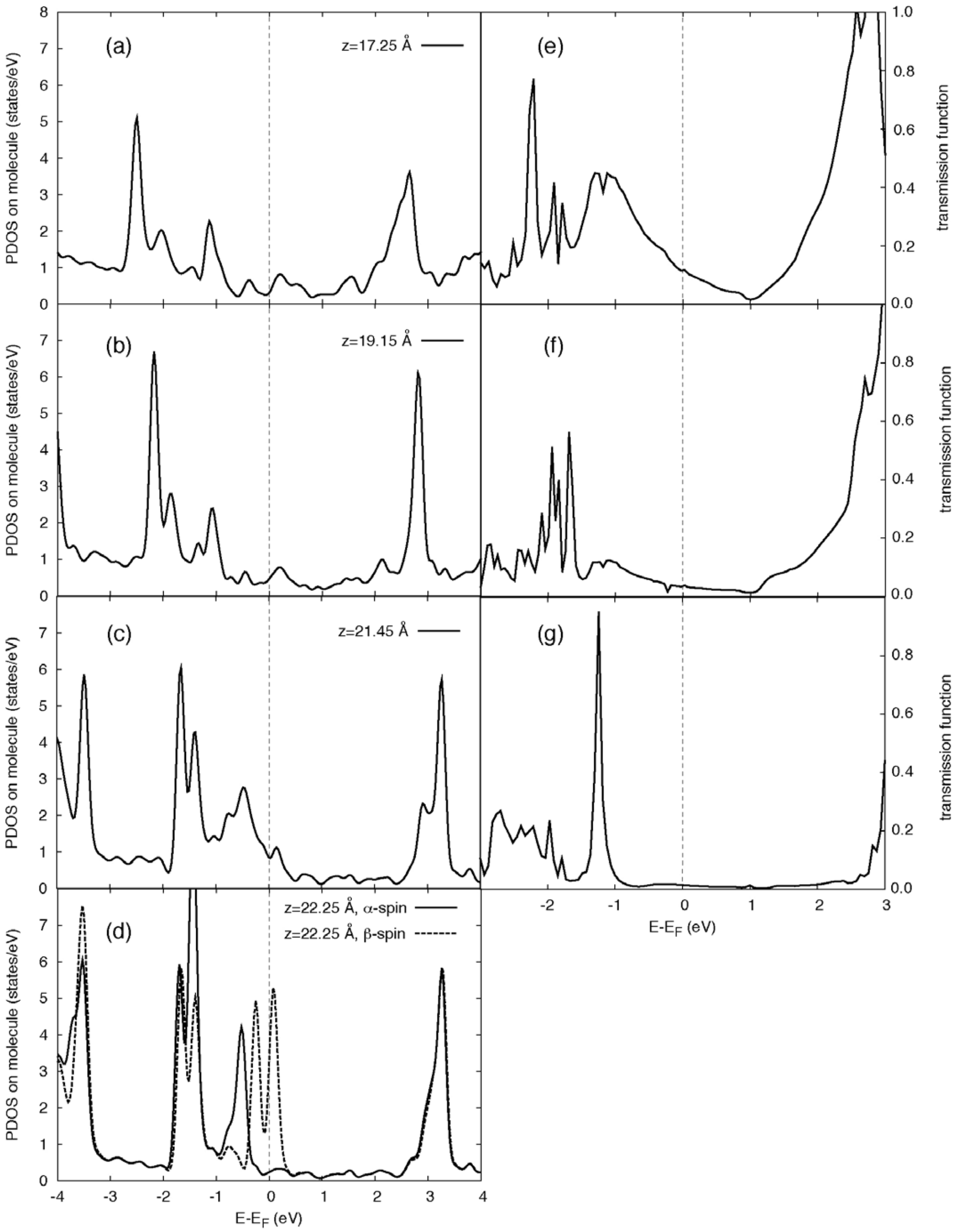

Figure 3. (a)–(d) PDOS on molecule and (e)–(g) transmission spectra for XYL junctions: (a), (e) a squeezed junction ($z = 17.25$ Å), (b), (f) the equilibrium junction length ($z = 19.15$ Å), (c), (g) just before the Au–S bond is broken ($z = 21.45$ Å) and (d) after the bond is broken ($z = 22.25$ Å). The transmission function was not evaluated for the latter case.

exactly to the energy minimum. Alternatively, F can be found by numerically differentiating the E versus z curve, but this makes the force very sensitive to a lack of smoothness in the energy curve.

The equilibrium length of the junction is $z = 19.15$ Å. Below this value the force is positive and acts in a direction to open the junction. Above $z = 19.15$ Å the force is negative, acting to close the junction. The minimum force is reached at $z = 21.45$ Å, when the sulfur–gold bond is broken. The breaking force of $|F| = 0.89$ eV Å^{-1}(=1.42 nN) is close to the value of 1.25 nN calculated in [11], where the gold–sulfur bond is also predicted to break before gold atoms are pulled out of the surface. For $z \geqslant 22.25$ Å when the bond is broken, the force returns to zero.

The projected density of states (PDOS) onto the orbitals centred at the molecular atoms is shown in figures 3(a)–(d) for different junction lengths. The two highest lying occupied states move closer to the Fermi level as the junction is stretched. When the bond is broken the α-spin and β-spin states are distinct (figure 3(d)). There is one less occupied β-spin state and hence the two pertinent β-spin states straddle the Fermi level.

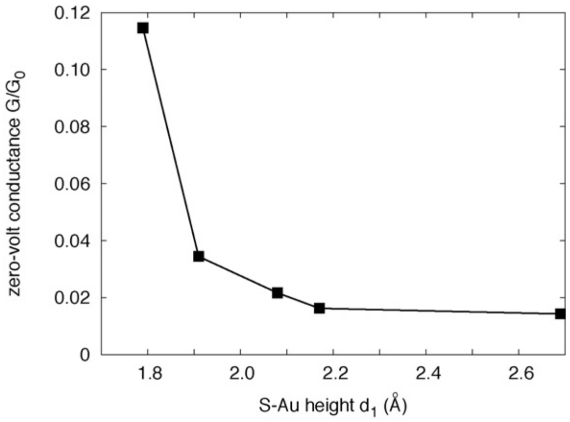

Figure 4. Zero volt conductance of the XYL junction for different unit cell lengths, z, as a function of the lower Au–S distance, d_1. The conductance was only calculated for spin singlet states where the Au–S bond is stretched, but not broken.

The transmission spectra (figures 3(e)–(g)) and hence 0 V conductances were calculated for some cell lengths with the SMEAGOL code. The conductance is shown in figure 4 as a function of the S–Au height, d. The conductance values have been normalized to the quantum of conductance G_0 equal to 77.48 μs. The conductance decreases as d_1 increases prior to bond breaking, in contrast to the behaviour in [7]. The present transport calculations are limited to spin-unpolarized ones and cannot reproduce bond breaking. The former calculations, however, were spin polarized and could be applied both before and after bond breaking. We have attempted spin-polarized transport calculations in the present case after the Au–S bond is broken but have been unable to obtain a converged self-consistent Hamiltonian. However, the (spin-polarized) PDOS peaks in figure 3(d) close to the Fermi level suggest that a transmission resonance will lie very close to the Fermi level and produce an enhanced conductance for β-spin electrons.

The sharp transmission resonance in figure 3(g) is presumably due to a combination of the weak coupling on one end and strong coupling on the other end of the junction. The resonance is located away from the Fermi level, so that the 0 V conductance is not affected.

It is surprising that in the squeezed junction with z = 17.25 Å (d_1 = 1.8 Å) the conductance is a factor of three larger than in the equilibrium case. The PDOS on the molecule is very similar in the vicinity of the Fermi level (compare figures 3(a) and (b)) and the enhanced conductance is not due to a resonance in the PDOS. The broad feature in the transmission spectrum around the Fermi level is enhanced when the junction is squeezed (compare figures 3(e) and (f)). This is presumably due to enhanced overlap between the sulfur and gold orbitals. The Mulliken overlap population on either side of the junction between the sulfur and each of the two bonded gold atoms is 0.17$|e|$ for the equilibrium junction and 0.19$|e|$ for the squeezed junction.

3.2. Au(111)–DEB–Au(111) junction

The DEB junction is shown in figure 5 at various stages of stretching. The equilibrium junction geometry (panel (b)) has a unit cell length of z = 18.25 Å. The carbon atoms on either end of the molecule were initially placed in fcc sites

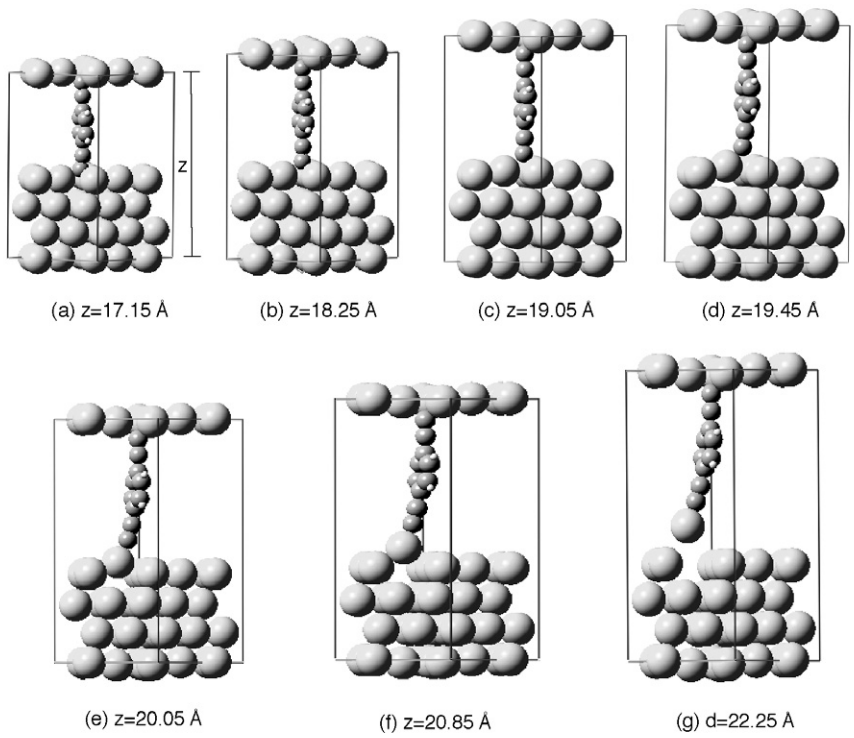

Figure 5. Unit cell lengths of the Au(111)–DEB–Au(111) junction at selected intervals of stretching. The equilibrium junction geometry is shown in panel (b) where z = 18.25 Å.

Table 2. Geometric parameters for relaxed DEB junctions. d_1 is the height of the carbon above the gold atom being pulled out of the surface. ΔAu_1 is the height of this gold atom above the rest of the surface. d_2 is the height of the carbon atom at the upper end of the molecule below the three gold atoms on the top surface to which it is bonded. ΔAu_2 is the distance of these three atoms below the rest of the top surface layer. z_{C-C} is the distance between the carbon atoms on opposite ends of the DEB molecule along the z-axis.

z (Å)	d_1 (Å)	ΔAu_1 (Å)	ΔAu_2 (Å)	d_2 (Å)	z_{C-C} (Å)
17.15	0.92	−0.02	−0.03	0.93	8.04
17.45	1.04	−0.01	0.00	1.02	8.10
17.75	1.13	0.02	0.03	1.11	8.16
18.05	1.19	0.05	0.08	1.22	8.22
18.25	1.29	0.10	0.08	1.23	8.27
18.45	1.33	0.15	0.11	1.28	8.30
18.75	1.44	0.21	0.14	1.32	8.35
19.05	1.53	0.27	0.17	1.39	8.40
19.45	1.75	0.39	0.20	1.42	8.38
19.85	1.84	0.78	0.22	1.42	8.29
20.05	1.87	0.95	0.22	1.43	8.29
20.25	1.88	1.13	0.23	1.43	8.29
20.45	1.92	1.28	0.22	1.43	8.30
20.85	1.93	1.62	0.23	1.45	8.30
21.25	1.94	1.95	0.25	1.47	8.31
21.65	1.93	2.32	0.26	1.49	8.31
21.85	1.92	2.53	0.28	1.50	8.31
22.25	1.86	3.01	0.31	1.49	8.25

on the surfaces at heights of 1.3 Å, the optimized position for adsorption on a single surface [26]. After optimization of the $z = 18.25$ Å junction, the three gold atoms bonded to each carbon move out of registry with the surface by $\Delta Au = 0.1$ Å. The heights of the carbons above these gold atoms are slightly reduced from 1.3 Å, but the carbon atoms remain in the same binding sites.

The ethynyl endgroups are more rigid than the methanethiol endgroups of XYL. The junction can be squeezed by 1.1 Å to $z = 17.15$ Å, but any further reduction in the unit cell length did not lead to a converged solution.

When the junction is stretched, a single gold atom is pulled out of the surface. As a result, the system remains in a spin singlet state throughout the stretching process. The strong carbon–gold bond, with a higher interaction energy than the sulfur–gold bond, does not break during stretching. However, the carbon is initially placed in a threefold hollow site and in the stretched geometry (figures 5(d)–(g)) it is bound only to the single gold atom detached from the surface. In molecular dynamics simulations of a thiolate molecule, a chain of gold atoms was predicted to be pulled out of the surface [20]. In order to simulate such behaviour, multiple layers of gold atoms would need to be relaxed. A larger unit cell with many more gold atoms would be needed, resulting in a much more computationally intensive study. The basic criterion for the extraction of a gold chain—breakage of the Au–Au bond before the Au–C bond—is met in the current calculations.

The geometric parameters of the junction at various unit cell lengths are defined in the same way as for XYL and summarized in table 2. ΔAu_1 and d_1 are measured with respect to the single gold atom pulled out of the surface. ΔAu_2 and d_2 are measured with respect to the three gold atoms closest to the carbon atom at the upper end of the molecule.

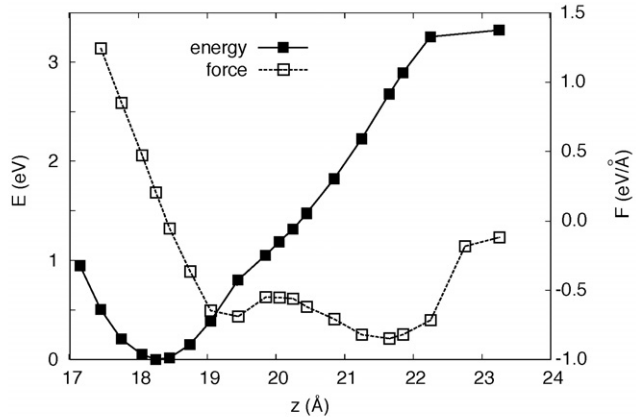

Figure 6. Relative total energy, E, and force, $F = -dE/dz$, versus unit cell length, z, for the DEB junction.

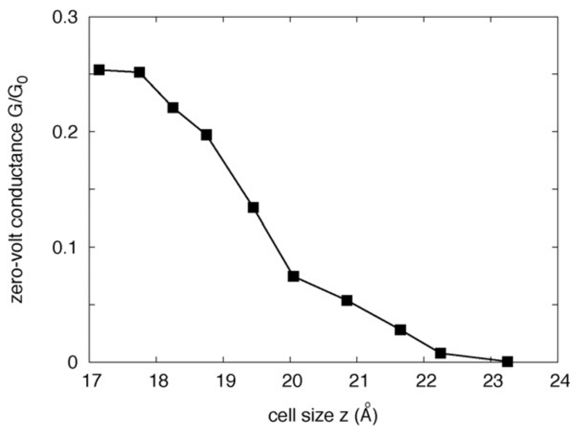

Figure 7. Zero volt conductance for the DEB junction as a function of unit cell length, z.

Figure 6 shows the total energy of the junction and the force, $F = -dE/dz$, on the unit cell length as a function of z. The limiting value of σ_{zz} was not explicitly calculated, but since the electrode geometry is identical to the XYL case the same value of $R = 0.17$ eV Å^{-1} was used as the residual stress.

The equilibrium unit cell length is $z = 18.25$ Å. Below this length the force is positive and acts to increase z. Above the equilibrium value the force is negative, acting to reduce z. Two minima can be identified for the force. The first minimum, $|F(19.45\ \text{Å})| = 0.69$ eV Å^{-1} = 1.10 nN, is the force required to pull the gold atom out of registry with the rest of the surface and reduce the number of gold atoms coordinated to the carbon atom from three to one. The second minimum, $|F(21.65\ \text{Å})| = 0.85$ eV Å^{-1} = 1.36 nN, is the force required to break the Au–Au bond and pull the single gold atom free from the surface. Since stretching the XYL junction did not succeed in pulling a gold atom free from the surface, it is surprising that the Au–Au breaking force calculated here is smaller than the S–Au breaking force calculated in the XYL case.

The 0 V conductance of the DEB junction is plotted in figure 7 as a function of the unit cell length, z. The conductance

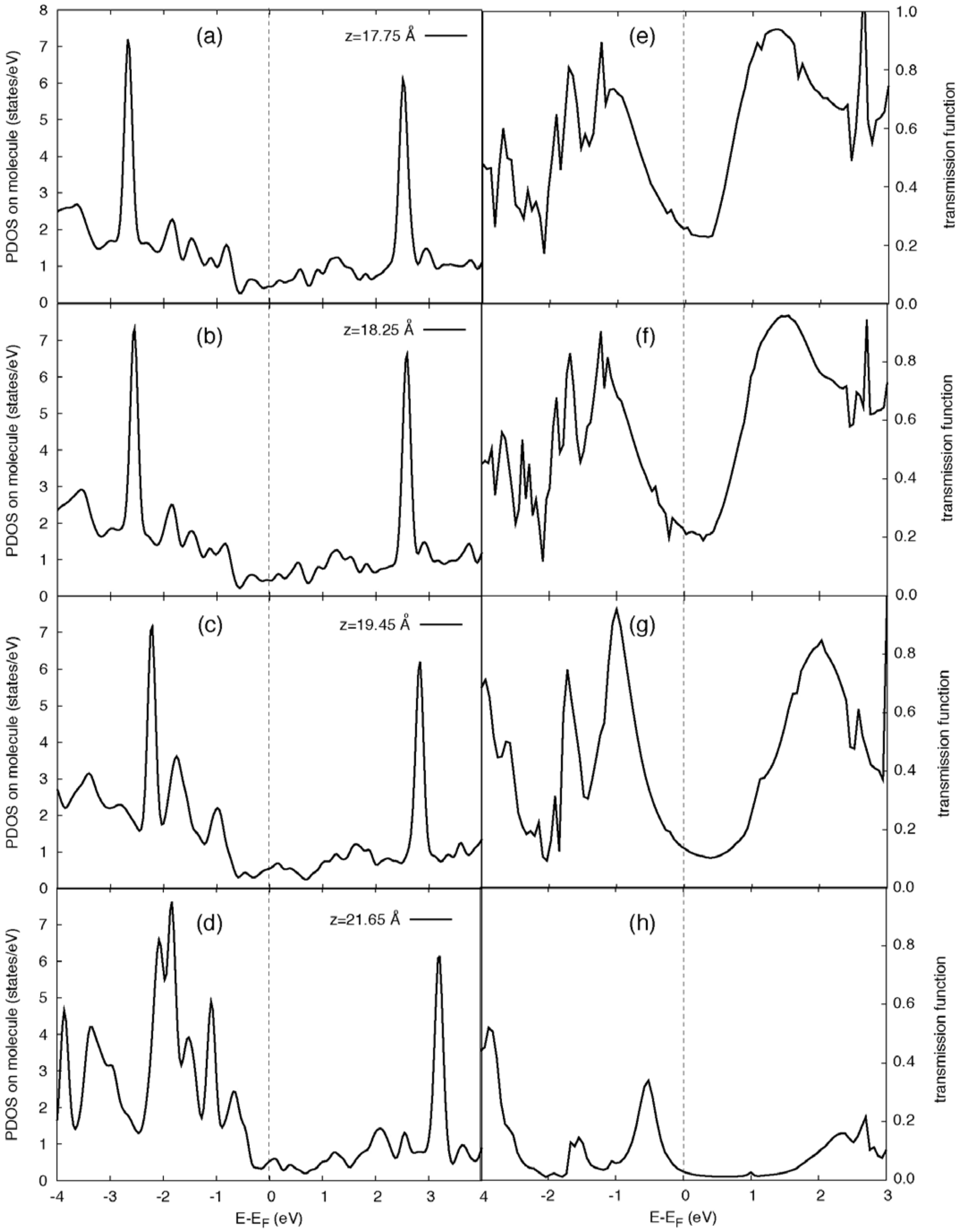

Figure 8. (a)–(d) PDOS on the DEB molecule including the detached gold atom. (e)–(h) Transmission functions for various junction lengths.

decays rapidly both initially, as the carbon atom is detached from the surface and binds to a single gold atom, and finally, as the gold atom is detached from the surface. The conductance is higher for the squeezed than the equilibrium junction.

The PDOS on the DEB molecule *including* the detached gold atom is plotted in figures 8(a)–(d) for various junction lengths. The corresponding transmission functions are shown in figures 8(e)–(h). Changes in the PDOS upon stretching are significant only for energies more than 1 eV below the Fermi level. The lowering of the broad transmission feature around E_F for the stretched junctions is due to the reduced coupling between the carbon and gold atoms as well as between the detached gold atom and the rest of the surface. The transmission resonance close to the Fermi level in the XYL case is not observed here since the Au–C bond is not broken and there are no unpaired electrons giving rise to states close to the Fermi level.

4. Conclusion

The geometries of benzenedimethanethiol (XYL) and ethynylbenzene (DEB) junctions with Au(111) electrodes were investigated as the junctions were systematically stretched and optimized in a series of steps. In the XYL junction, the Au–S bond was cleaved before any gold atoms were removed from the surface. The force required to break this bond was calculated as 1.42 nN, slightly larger than previous estimations [11]. The conductance decreased as the junction was stretched and increased as the junction was squeezed from its equilibrium geometry. Once the Au–S bond is broken, the junction is in a spin doublet state. In this case spin-polarized calculations are necessary. We were unable to calculate the transmission function for the spin-polarized system, but a converged electronic structure was obtained. A resonance in the density of states projected onto the XYL molecule occurs close to the Fermi level only for electrons of one spin type. This suggests that an enhanced conductance may be obtained for electrons of one spin type over the other, as predicted in previous work [7].

A similar analysis was performed for the Au(111)–DEB–Au(111) junction. This junction is more conductive and the Au–C bond is predicted to be stronger than the Au–S bond. The Au–C bond was not broken as the junction was stretched; however, the carbon changes from initial attachment to a threefold hollow site to being bound to a single gold atom. This gold atom is detached from the rest of the surface upon stretching. Accordingly, there are two peaks in the force versus unit cell length curve. The first, $F_1 = 1.10$ nN, corresponds to the change in the nature of the Au–C interaction. The second, $F_2 = 1.36$ nN, corresponds to breaking of the Au–Au bond. The presence of the gold bonded to the terminal carbon precludes a resonance in the PDOS and transmission function and hence the conductance decays rapidly as the DEB junction is stretched.

This analysis shows that the nature and strength of the interaction between the molecule and electrode can have a significant effect on the conductance response of a stretched molecular junction.

References

[1] Joachim C, Gimzewski J K and Aviram A 2000 *Nature* **408** 541
[2] Hush N 2003 *Nat. Mater.* **2** 134
[3] Lindsay S M and Ratner M A 2007 *Adv. Mater.* **19** 23
[4] Akkerman H B, Blom P W M, de Leeuw D M and de Boer B 2006 *Nature* **441** 69
[5] Hoft R C, Armstrong N, Ford M and Cortie M B 2007 *J. Phys.: Condens. Matter* **19** 215206
[6] Basch H, Cohen R and Ratner M A 2005 *Nano Lett.* **5** 1668
[7] Hoft R C, Ford M J and Cortie M B 2006 *Chem. Phys. Lett.* **429** 503
[8] Hu Y B, Zhu Y, Gao H J and Guo H 2005 *Phys. Rev. Lett.* **95** 156803
[9] Ke S H, Baranger H U and Yang W T 2005 *J. Chem. Phys.* **122** 074704
[10] Muller K H 2006 *Phys. Rev.* B **73** 045403
[11] Romaner L, Heimel G, Gruber M, Bredas J L and Zojer E 2006 *Small* **2** 1468
[12] Solomon G C, Reimers J R and Hush N S 2005 *J. Chem. Phys.* **122** 224502
[13] Speyer G, Akis R and Ferry D K 2003 *Superlatt. Microstruct.* **34** 429
[14] Speyer G, Akis R and Ferry D K 2005 *IEEE Trans. Nanotechnol.* **4** 403
[15] Xue Y Q and Ratner M A 2003 *Phys. Rev.* B **68** 115407
[16] Delaney P and Greer J C 2004 *Phys. Rev. Lett.* **93** 036805
[17] Sai N, Zwolak M, Vignale G and Di Ventra M 2005 *Phys. Rev. Lett.* **94** 186810
[18] Solomon G C, Reimers J R and Hush N S 2004 *J. Chem. Phys.* **121** 6615
[19] Xu B Q and Tao N J J 2003 *Science* **301** 1221
[20] Kruger D, Fuchs H, Rousseau R, Marx D and Parrinello M 2002 *Phys. Rev. Lett.* **89** 186402
[21] Ordejon P, Artacho E and Soler J M 1996 *Phys. Rev.* B **53** 10441
[22] Soler J M, Artacho E, Gale J D, Garcia A, Junquera J, Ordejon P and Sanchez-Portal D 2002 *J. Phys.: Condens. Matter* **14** 2745
[23] Troullier N and Martins J L 1991 *Phys. Rev.* B **43** 1993
[24] Perdew J P, Burke K and Ernzerhof M 1996 *Phys. Rev. Lett.* **77** 3865
[25] Monkhorst H J and Pack J D 1976 *Phys. Rev.* B **13** 5188
[26] Ford M J, Hoft R C and McDonagh A 2005 *J. Phys. Chem.* B **109** 20387
[27] Rocha A R, Garcia-Suarez V M, Bailey S, Lambert C, Ferrer J and Sanvito S 2006 *Phys. Rev.* B **73** 085414
[28] Rocha A R, Garcia-Suarez V M, Bailey S W, Lambert C J, Ferrer J and Sanvito S 2005 *Nat. Mater.* **4** 335
[29] Datta S 1995 *Electronic Transport in Mesoscopic Systems* (Cambridge: Cambridge University Press)